

Possibility of a more detailed seismic interpretation within the Miocene formations of the Carpathian Foredeep based on the well logs interpretation

Możliwość uszczegółowienia interpretacji sejsmicznej w utworach miocenu zapadliska przedkarpackiego na podstawie interpretacji pomiarów geofizyki otwórowej

Andrzej Urbaniec, Marek Stadtmüller, Robert Bartoń

Oil and Gas Institute – National Research Institute

ABSTRACT: The main aim of the article is to determine the possibility of a more detailed seismic interpretation in the autochthonous Miocene formations on the example of a 3D seismic survey from the Carpathian Foredeep area, based on the comprehensive analysis of well logs. The seismic survey located in the central part of the Carpathian Foredeep was selected for the study. This zone is characterized by the presence of natural gas accumulation in various types of traps. Four boreholes in which formation tests were conducted within the Miocene sediments were selected for the detailed interpretation of the well logs. An important element of the study was the seismic-to-well tie based on available measurements of vertical seismic profiling. The quantitative interpretation of well data was the basis for the distinction of several lithofacial complexes of diverse lithology, reservoir parameters, or the type of reservoir media saturation in the profile of each of the analysed wells. Water and hydrocarbon saturations were estimated based on Montaron's theory. With the defined seismic signature, it was possible to interpret seismic horizons away from the wells. Selected seismic attributes were used during the interpretation and analysis of the seismic image. There was a fairly high correlation between the well logs interpretation and the seismic record. Major lithological changes, thicker claystone interbeds within mudstone, or heterolithic deposits, as well as zones of significant changes in reservoir properties and the type of reservoir media saturation can be interpreted in the seismic image. In contrast, mudstone or heterolithic complexes of a large thickness (about hundreds of meters) in the seismic image are usually characterized by a monotonous low amplitude record and a significantly smaller continuity of reflections. The zones saturated with gas or gas and brine, documented in the analysed wells by the results of formation tests, usually can be identified on the basis of the seismic record. Due to the large variation of lithology and a substantial variability of individual parameters, it is not possible to reliably indicate in the seismic data which of the analysed objects are saturated with natural gas, and which with gas and brine. The results of well logs and integrated seismic interpretation allowed to obtain the complete picture of the Miocene siliciclastic formations diversity in the studied region, as well as a more accurate determination of reservoir properties and reservoir fluid saturation. The series of fine-grained sediments (mainly mudstone or heterolithic) in the lower part of the Miocene profile, within which several prospects were interpreted, was determined as the most interesting for hydrocarbon exploration.

Key words: Miocene of the Carpathian Foredeep, VSP, Montaron's method, seismic interpretation, seismic attributes.

STRESZCZENIE: Zasadniczym celem artykułu jest określenie możliwości uszczegółowienia interpretacji sejsmicznej w utworach miocenu autochtonicznego, na przykładzie zdjęcia sejsmicznego 3D z obszaru zapadliska przedkarpackiego, na podstawie kompleksowej analizy profilowań geofizyki otwórowej. Do badań wytypowano zdjęcie sejsmiczne z centralnej części zapadliska, ze strefą cechującą się obecnością akumulacji gazu ziemnego w różnego typu pułapkach złożowych. Do szczegółowej interpretacji profilowań geofizyki otwórowej wybrane zostały cztery otwory wiertnicze, w których prowadzono próby złożowe w obrębie utworów miocenu. Istotnym elementem opracowania było dowiązanie danych otworowych do obrazu sejsmicznego w oparciu o dostępne pomiary pionowego profilowania sejsmicznego. Ilościowa interpretacja danych geofizyki wiertniczej stanowiła podstawę do wyodrębnienia w profilu każdego z analizowanych otworów szeregu kompleksów facjальных, o zróżnicowanej litologii, parametrach zbiornikowych czy też rodzaju nasycenia mediani złożowymi. Nasycenie mediani złożowymi szacowano na podstawie teorii Montarona. Dla wyodrębnionych kompleksów próbowało odnaleźć odpowiedź w zapisie sejsmicznym, a następnie, o ile było to możliwe, prześledzić ich zasięg przestrzenny. W trakcie interpretacji i analizy obrazu sejsmicznego opierano się przede wszystkim na wersjach sejsmiki w odtworzeniu

Corresponding author: A. Urbaniec, e-mail: andrzej.urbaniec@inig.pl

Article contributed to the Editor 14.02.2019. Approved for publication 6.08.2019.

wybranych atrybutów sejsmicznych. Stwierdzono dosyć dużą zgodność interpretacji profilowań geofizyki otworowej z zapisem sejsmicznym. Najwyraźniej w zapisie tym zaznaczają się strefy dużych zmian litologicznych, bardziej małysze wkładki ilowców w obrębie mułowców lub heterolitów, jak również strefy wyraźnych zmian właściwości zbiornikowych i nasyceń mediami złożowymi. Natomiast kompleksy mułcowe lub heterolitowe o dużej małyszości (rzędu setek metrów) w obrazie sejsmicznym cechują się najczęściej monotonnym, niskoamplitudowym zapisem oraz wyraźnie mniejszą ciągłością refleksów. Udokumentowane wynikami prób złożowych w analizowanych otworach strefy nasycone gazem lub gazem z solanką na ogół mogą być identyfikowane na podstawie zapisu sejsmicznego. Ze względu na duże zróżnicowanie litologiczne i znaczny zakres zmienności poszczególnych parametrów nie ma możliwości wiarygodnego wytypowania na podstawie samego zapisu sejsmicznego, które z analizowanych obiektów nasycone są gazem ziemnym, a które gazem z domieszką solanki. Wyniki kompleksowej interpretacji geofizyki wiertniczej i sejsmiki pozwolą na uzyskanie możliwie pełnego obrazu zróżnicowania facjalnego klastycznych utworów miocenu w badanym rejonie, jak również na dokładniejsze określenie właściwości zbiornikowych i charakterystyki nasycenia plynami złożowymi. Za najbardziej interesujący pod kątem poszukiwania złóż węglowodorów uznano pakiet drobnoklastycznych utworów (głównie mułcowych lub heterolitowych) w niższej części profilu miocenu, w obrębie którego wyinterpretowano szereg obiektów potencjalnie nasyconych gazem ziemnym.

Słowa kluczowe: miocen zapadliska przedkarpackiego, PPS, metoda Montarona, interpretacja sejsmiczna, atrybuty sejsmiczne.

Introduction

The aim of the presented thesis was to define the possibility of providing a more detailed seismic interpretation in the autochthonous Miocene strata, within a chosen 3D seismic survey from the Carpathian Foredeep. A 3D seismic survey from the central part of the Foredeep, obtained by joint processing of two seismic surveys, i.e. the new survey "A" of 2015 and the archival survey "B" (fig. 1), was chosen for the research. Natural gas accumulations located in various kinds of traps were found in the Miocene sediments in this region (Karnkowski, 1993).

For a detailed interpretation of well logs, four boreholes were selected, all within the seismic survey "A" (fig. 1), in which formation tests in the Miocene sediments were conducted:

- Borehole "O", the newest in the analysed region, with a complete set of geophysical logs and one tested interval within the Miocene sediments, out of which a supply of natural gas was obtained;
- Borehole "J" with two tested intervals within the Miocene sediments, where gas with brine flow was obtained;
- Borehole "ZA" with four tested intervals within the Miocene sediments, where brine with gas shows (from two intervals), brine (from two intervals) or no flow were documented;
- Borehole "ZU" with five tested intervals that were tested within the Miocene sediments, with low flow of natural gas or gas with brine, and in the case of one interval with no flow at all.

An outline of the region's geological structure

The sedimentary basin of the Carpathian Foredeep developed in the Carpathian Foreland was a fragment of a large foreland graben basin stretching along the whole Carpathian arc. The complex of autochthonous Miocene strata in the analysed region can be divided into three basic litho-stratigraphic units:

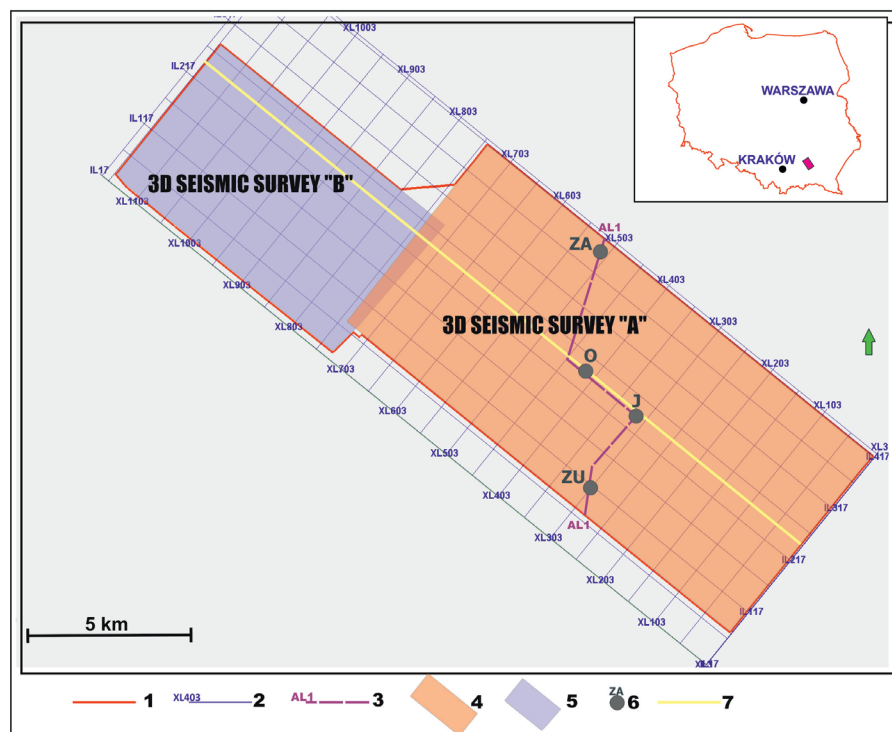


Fig. 1. Localization and outlines of analysed 3D seismic surveys; 1 – outlines of a collated 3D seismic survey, 2 – seismic lines and traces, 3 – arbitrary line joining the analysed boreholes, 4 – new seismic survey "A", 5 – seismic survey "B" after reprocessing, 6 – the boreholes in which the interpretation of well logs was conducted, 7 – line of the geological cross-section (fig. 2)

Rys. 1. Lokalizacja i zarysy analizowanych zdjęć sejsmicznych 3D; 1 – kontury połączonych zdjęć sejsmicznych 3D, 2 – linie i trasy sejsmiczne, 3 – linia arbitralna łącząca analizowane odwierty, 4 – nowe zdjęcie sejsmiczne „A”, 5 – zdjęcie sejsmiczne po reprocessingu „B”, 6 – otwory wiertnicze, w których wykonano interpretację pomiarów geofizyki otworowej, 7 – przebieg przekroju geologicznego (rys. 2)

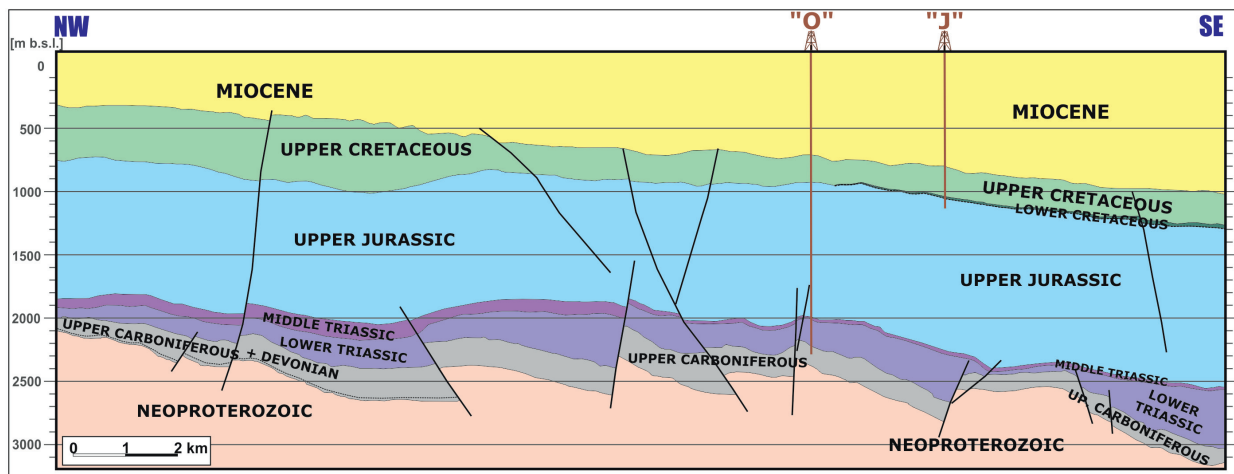


Fig. 2. Geological cross-section of the investigated region (localization – see fig. 1)

Rys. 2. Przekrój geologiczny przez obszar badań (lokalizację przekroju przedstawiono na rys. 1)

the clastic subevaporite series, the evaporite series of Upper Badenian and the Upper Badenian and Sarmatian clastic series.

The subevaporite sediments are mainly represented by a set of claystones and mudstones of the Skawina formation, with thickness ranging from a dozen to a few dozen meters. The genesis of the Badenian evaporite series is connected with the so-called Badenian Salinity Crisis (BSC) probably commenced by a rather sudden drop of sea level due to global cooling (Oszczypko, 2006; Bukowski, 2011). Within the analysed seismic survey region there occur sulphate rocks, i.e. gypsum and anhydrite, distinguished as the Krzyżanowice formation (Alexandrowicz et al., 1982; Olszewska, 1999). The siliciclastic sediments classified as the Machów formation (Alexandrowicz et al., 1982) are an essential part of the autochthonous Miocene profile in the analysed region of the Carpathian Foredeep. This formation is characterized by a considerable lithologic heterogeneity and built of sandstone-claystone-mudstone sediments appearing in the profile in different proportions and of significantly high facies diversity.

The middle stage is composed of Meso-Paleozoic rocks of a considerable summary thickness up to 2000 m (fig. 2). The lowest structural stage recognized in the profiles of deep boreholes is a series of Neoproterozoic anchimetamorphic rocks (fig. 2), originally connected with the structure of the Małopolska Block (Buła et al., 2008).

Construction of synthetic seismograms with the use of VSP measurements

The seismic-to-well tie was completed upon the basis of recorded vertical seismic profiling (VSP) in the zero-offset version, in boreholes chosen for a detailed analysis based on calculated synthetic seismograms. Upon the VSP data recorded

in the zero-offset version it was possible to define the hodograms of the first arrival compressional wave in full range of the conducted measurements. These hodograms were used to construct synthetic seismograms, to define the true depth-time relation and, what follows, to determine the accurate correlation of stratigraphic boundaries and interval velocities with seismic reflective boundaries (Brewer, 2002).

Due to the limited scope of this work, only the example of seismic-to-well tie for the "O" borehole will be discussed. In this borehole, a VSP zero-offset type measurement set 68 m from the borehole and at azimuth of 316° was carried out with the use of a vibratory source. The measurement step was 5 m.

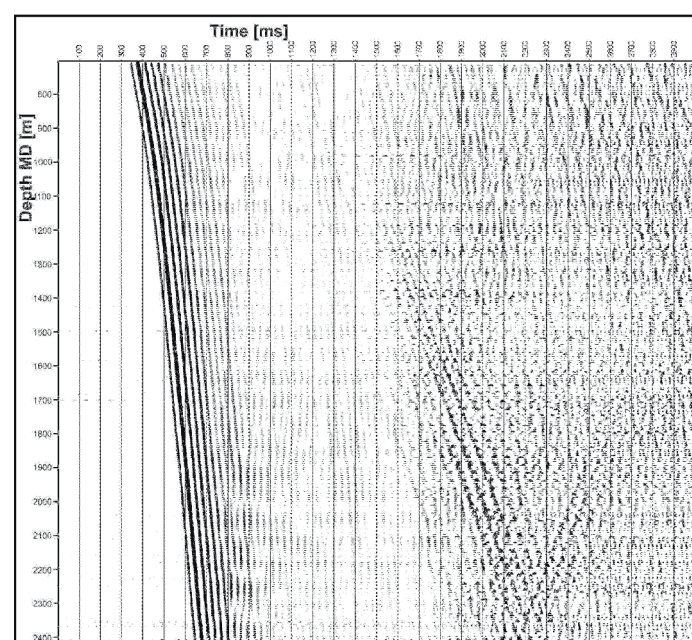


Fig. 3. Recorded VSP data for the vertical component in the "O" borehole after band filtering of high resonance frequencies

Rys. 3. Zarejestrowane dane PPS dla składowej pionowej w otworze „O” po filtracji pasmowej wysokich częstotliwości rezonansowych

Three-componential geophones were used for the VSP. The records obtained in an 2290–815 m interval are of a very good quality (fig. 3). Stabile, strong downgoing waves, weakening reflections from reflection boundaries can be observed. Neither significant disturbances, considerable shape changes of the incident wave signal nor any interference of the incident wave with other kinds of waves can be noticed (near the first impulse). The first impulses defined in that interval are fully reliable. In figure 4, the defined two-way time hodograph was presented together with the well logs: acoustic (DT) and density (RHOB), and with marked stratigraphic boundaries. These well logs were used for the synthetic seismogram calculations (fig. 5). The range of the amplitude spectrum of the zero-phase wavelet obtained from the seismic data in the neighbourhood of the “O” borehole is between 0 to 110 Hz (with a dominant frequency of 28 Hz). The synthetic seismogram calculated

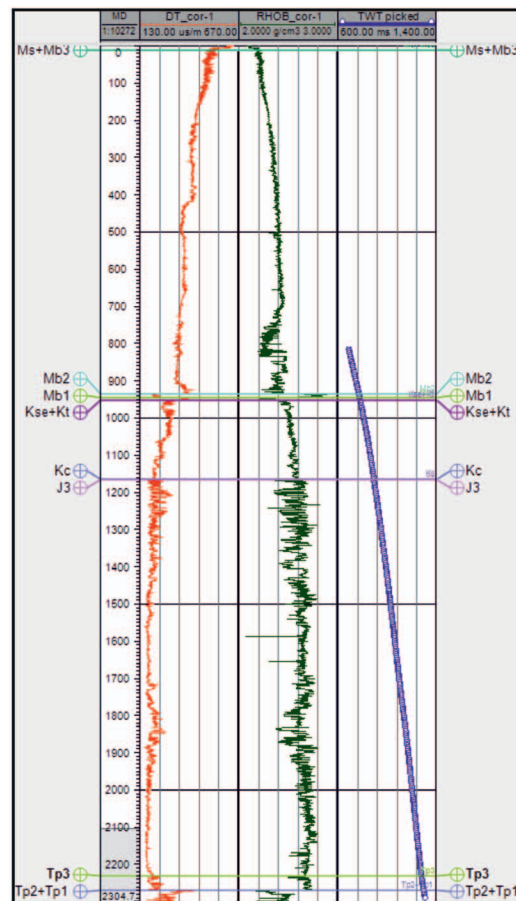


Fig. 4. A correlative set of DT acoustic and RHOB density logging with the hodogram of the first arrival compressional wave marked out in the VSP wave field of the “O” borehole

Rys. 4. Zestawienie korelacyjne pomiarów otworowych profilowania akustycznego DT i gęstości RHOB z hodografem pierwszych impulsów wyznaczonym na polu falowym PPS dla otworu „O”

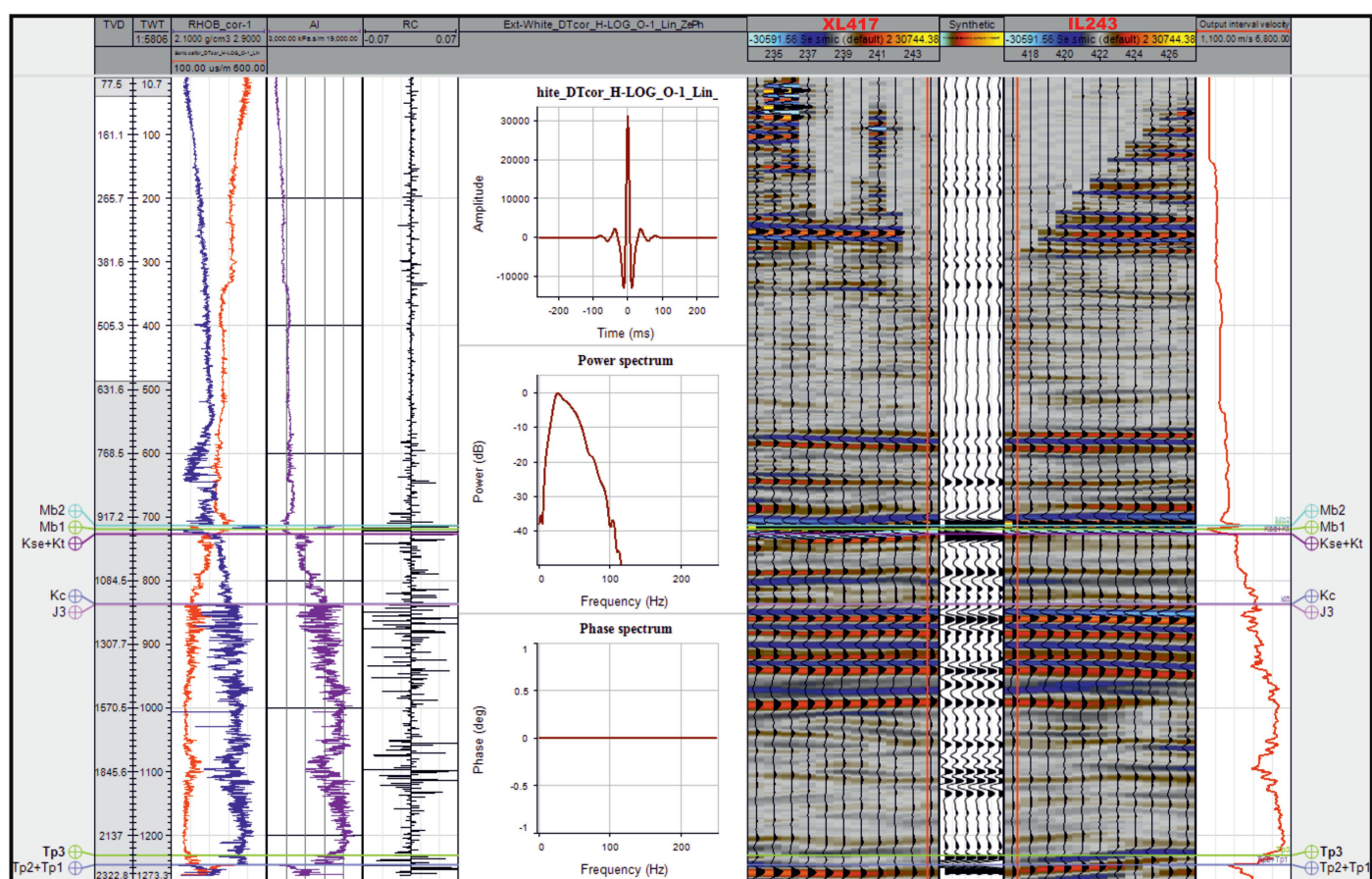


Fig. 5. A synthetic seismogram calculated for the “O” borehole

Rys. 5. Sejsmogram syntetyczny obliczony dla otworu “O”

with the use of the Petrel programme from Schlumberger was compared against seismic profiles in the location of the "O" borehole (IL243, XL417) (fig. 5). It is the necessary step for correlating the well logs' stratigraphic interpretation with a seismic record. The obtained result shows a very high quality of the correlation of the well logs with the seismic profiles.

Quantitative analysis of well logs

An analysis of the well log data, the integrity of the laboratory and the well tests results, with actual preparation of a quantitative petrophysical model of the autochthonous Miocene sediments in the studied region was conducted. The first stage of work included preparation of well logs for tying the seismic data with the borehole data. In the second stage, a complementary quantitative interpretation of mineral composition of the rock matrix and of reservoir media saturation was conducted with the use of the Montaron model.

A quantitative interpretation of mineral composition of the autochthonous Miocene sediments, porosity and permeability was conducted by applying both the classic techniques of neutron-acoustic crossplot and optimization algorithms, using TechLog and ProGeo programs on the assumed volumetric model:

$$\text{CLAY MINERALS CONTENT} + \text{QUARTZ} + \\ + \text{CARBONATES} + \text{POROSITY}$$

The results of which were calibrated on the laboratory material.

Additionally, an empiric relation was developed in the form of a correlation between the carbonates content Vcarb and the clay minerals content Vsh. Formula (1) presented as an exponential function correlates the laboratory data on the significance level of 0.567.

$$V_{\text{carb}} = 19,09 \cdot e^{-0,21} \cdot V_{\text{sh}} \quad (1)$$

Estimation of effective porosity PHI_ef was based on the further described concept of critical saturation Sc, as part of the porous space inaccessible to filtration with hydrocarbons, according to the formula (2).

$$\text{PHI_ef} = \text{PHIIT} - (S_c \cdot \text{PHIIT}) \quad (2)$$

Absolute permeability was estimated by utilising the power function calculated upon laboratory data following formula (3) with the significance level $R^2 = 0.785$.

$$K_{\text{cor}} = 13301 \cdot \text{PHI_ef} + 3.066 \quad (3)$$

Saturation with reservoir media has been estimated by using Bernard Montaron's theory (Montaron, 2008, 2009; Jarzyna

and Krakowska, 2010), which has already been tested by INIG – PIB in several industrial works in recent years. Water saturation according to Montaron's model can be calculated following formula (4) and formula (5).

$$R_t = R_w' / (S_w \cdot \varphi - WCI)^\mu \quad (4)$$

$$R_w' = R_w(1 - WCI)^\mu \quad (5)$$

where:

R_t – formation true resistivity,
 R_w' – apparent formation water resistivity,
 R_w – true formation water resistivity,
 φ – effective porosity,
 WCI – water connectivity index,
 μ – conductivity exponent,
 S_w – water saturation.

The full set of the Montaron model parameters also includes critical saturation S_c connected with the saturation parameter RI defined as a relation of formation resistivity unaltered by filtration (R_t) to that of a formation saturated in 100% with reservoir water (R_o), with the use of formula (6) and to water connectivity index WCI, with the use of formula (7).

$$RI = \left(\frac{1 - S_c}{S_w - S_c} \right)^\mu \quad (6)$$

$$S_c = \frac{WCI}{\varphi} \Rightarrow WCI = S_c \varphi \quad (7)$$

The above parameters are a group of effective parameters introduced upon the general theory EMT (Effective Medium Theory) allowing to simplify the description of a complicated rock structure, which in the case of water saturation gives a possibility to replace two parameters, m (compactness) and n (wettability), both depending on porosity and water saturation, with a single one: μ (water conductivity exponent), independent from those two parameters.

The application of former tests with the use of the Montaron model in practical interpretations of the Miocene autochthonic formations made it possible to choose proper values of the model's parameters: critical saturation S_c _PHI calculated as effective porosity function, formula (8) and conductivity exponent μ , the value of which in the case of all the well logs was contained within: 0.7–1.45 and allowed to estimate S_w _cor – water saturation appropriately to the obtained results of the formation tests.

$$S_c \text{ PHI} = -0.0306 \cdot \text{PHI_ef} + 0.9827 \quad (8)$$

An example of an interpretation of the lithology and petrophysical parameters for a Miocene profile in borehole "O" is presented in figure 6.

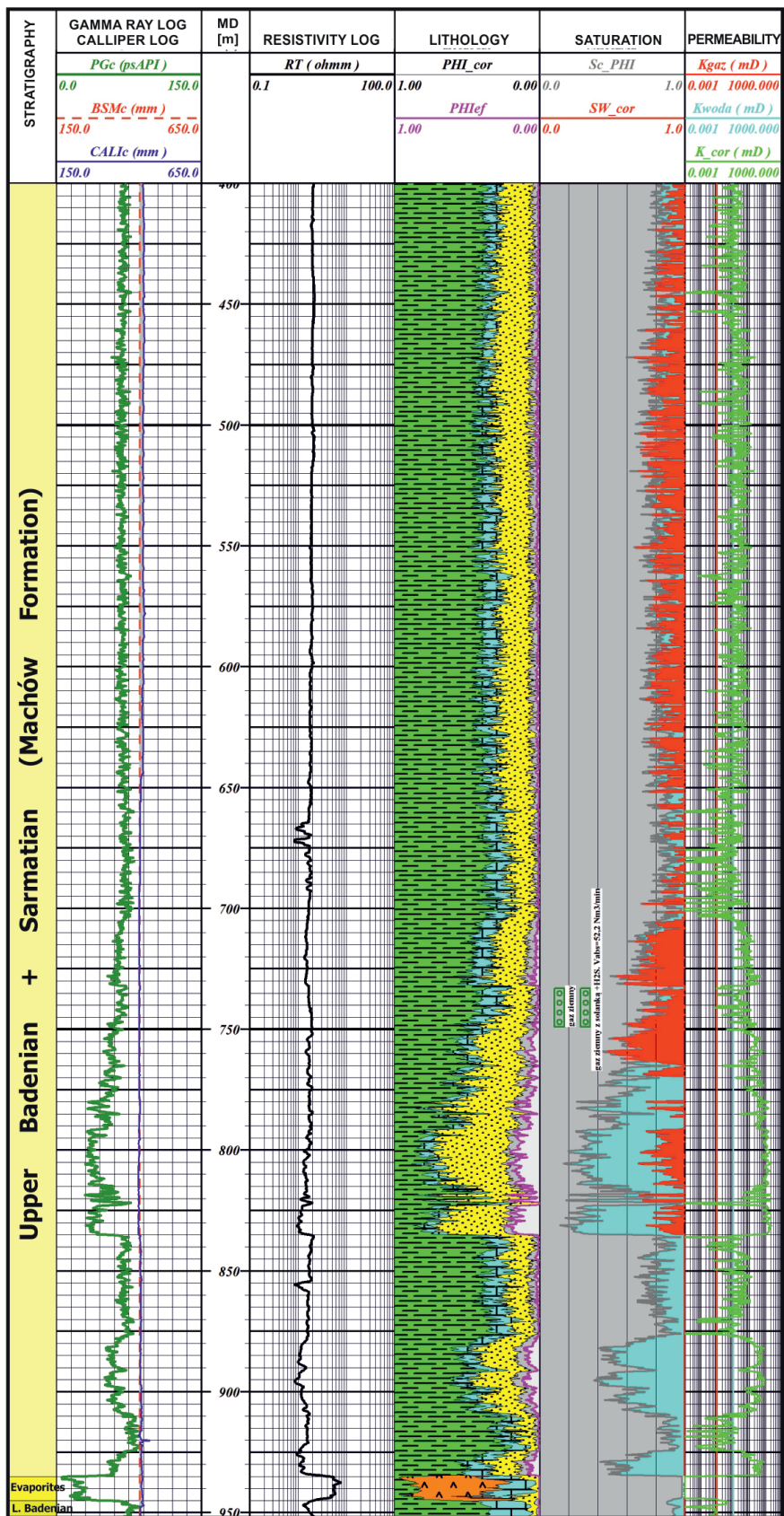


Fig. 6. An example of interpretation of lithology and petrophysical parameters in the Miocene autochthonic formations in the borehole "O" (lithology and saturation key as in fig. 7)

Rys. 6. Przykład wynikowej interpretacji litologii i parametrów petrofizycznych w utworach miocenu autochtonicznego dla otworu „O” (legenda dla litologii i nasycenia jak na rys. 7)

Distinction of lithofacial complexes in the Miocene formations

On the basis of an integrated interpretation of the well logs within the Miocene autochthonous formations, several units called "lithofacial complexes" were distinguished in the four selected boreholes. The main selection criterion of the mentioned complexes in the investigated profile was lithological variability; also other factors, such as porosity, permeability and type of saturation were considered.

Generally, among the selected units the following complexes were found:

- claystone complexes (i), usually of small thickness (up to a dozen or so meters);
- mudstone complexes (m) dominating in the analysed region, sometimes reaching considerable thickness (above 300 m);
- heterolithic complexes consisting mainly of fine-grained sediments (mudstones and claystones) (h) of very variable thickness of about a dozen to 300 m;
- heterolithic complexes consisting mainly of medium-grained sediments (sandstones and mudstones) (hp), with a thickness from 10 to 70 m;
- sandstone complexes (p) of varied thickness from several to maximum 75 m.

The complexes were named according to the following: abbreviation of the borehole name _type of selected complex (i,m,h,hp,p)_ successive number of the given complex in the borehole profile, for example O_hp_1. Lithofacial complexes distinguished in the Miocene sediments based on the example of a profile fragment from the borehole "ZA" are presented in figure 7.

The depths of the selected lithofacial complexes top surfaces in all four analysed boreholes were entered into the Petrel system. With the defined lithofacial complexes seismic interpretation was performed in the distance of several hundred meters from the particular borehole (fig. 8).

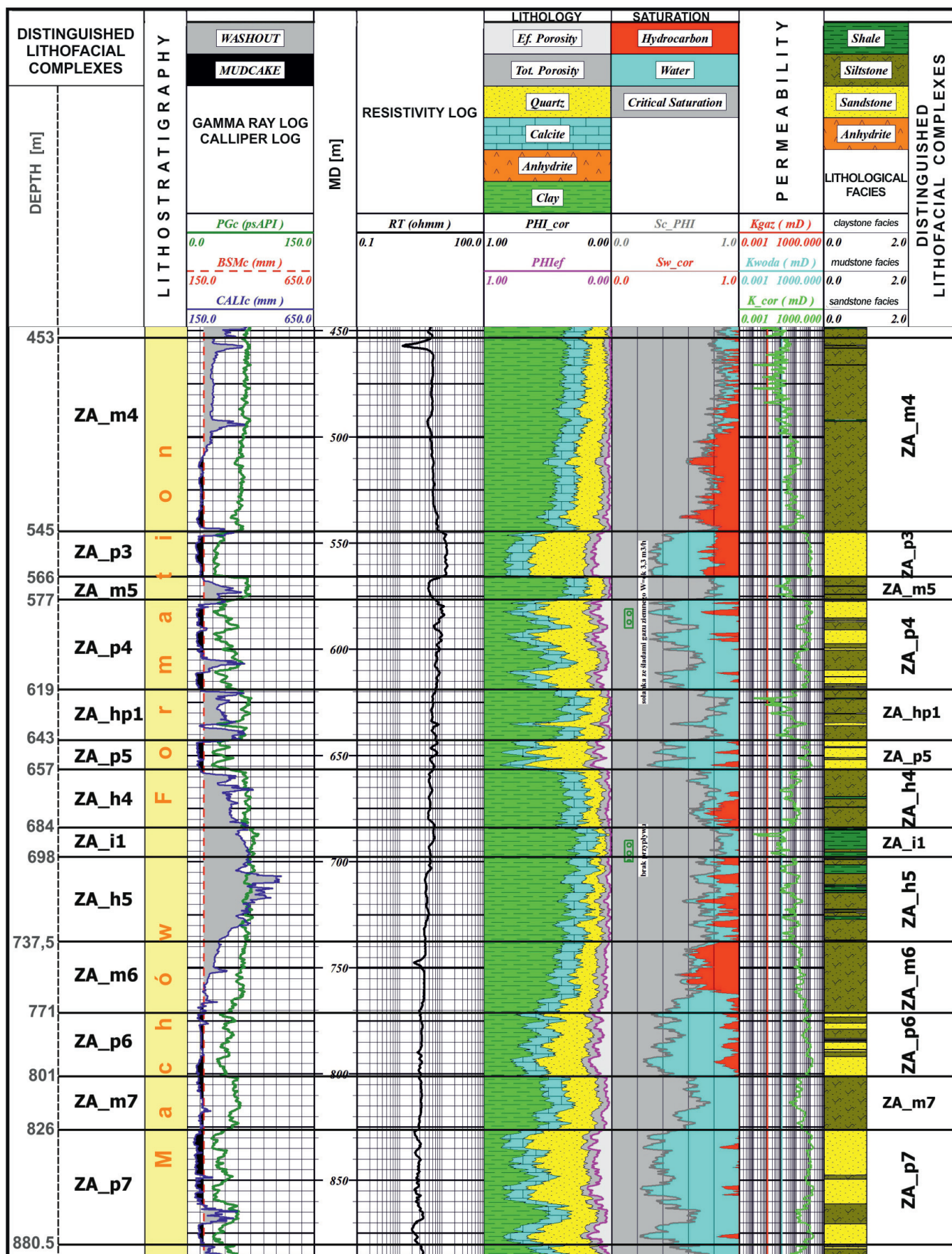


Fig. 7. Distinguished complexes in the Miocene sediments on the example of the “ZA” borehole profile

Rys. 7. Wydzielenia kompleksów facjalnych w utworach miocenu na przykładzie fragmentu profilu otworu ZA

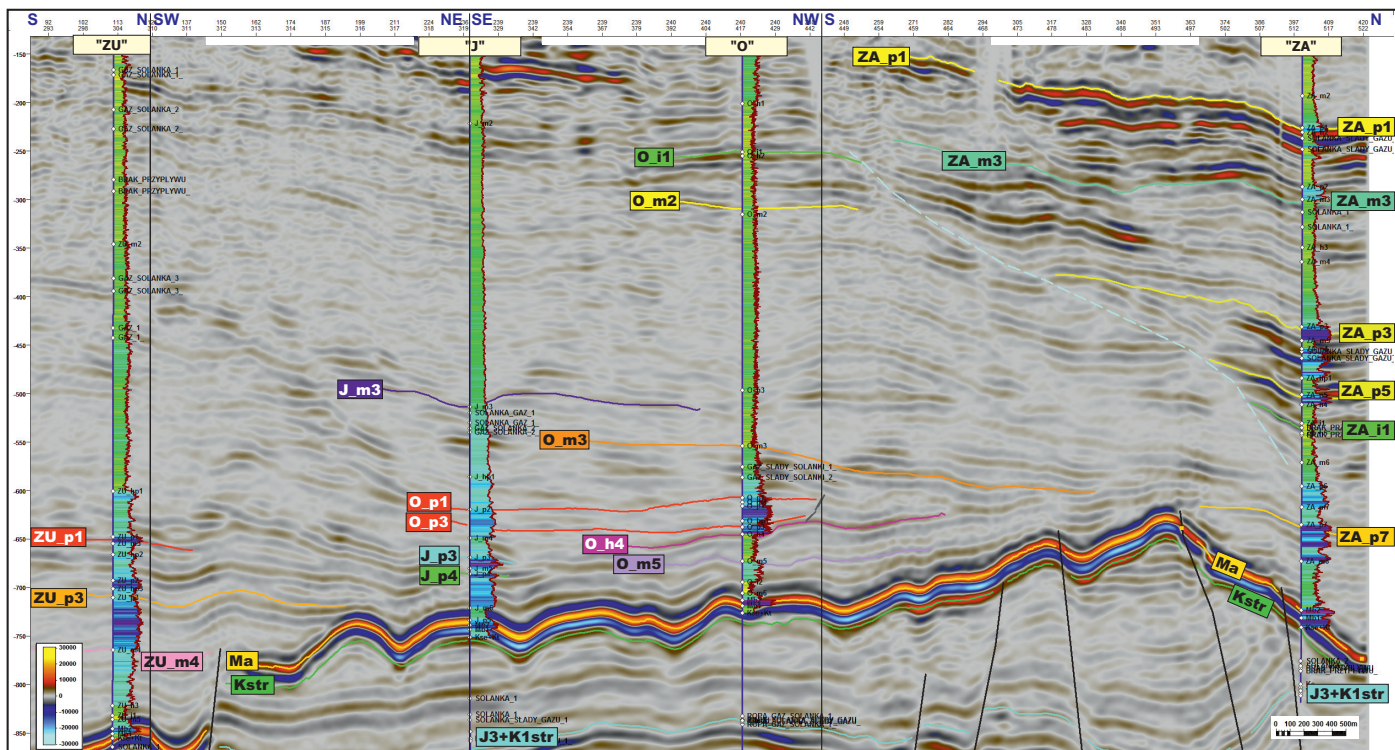


Fig. 8. Seismic time section AL1 connecting the analysed boreholes (localization of the section shown in figure 1), with calculated clay content profiles in particular boreholes; Ma – the top of Badenian evaporites, Kstr – the top of Upper Cretaceous sediments, J3+K1str – the top of Lower Cretaceous – Upper Jurassic sediments, other abbreviations – tops of interpreted complexes distinguished in Miocene profiles in particular boreholes

Rys. 8. Czasowy przekrój sejsmiczny AL1 łączący analizowane otwory wiertnicze (lokalizację przekroju przedstawiono na rys. 1) w zestawieniu z obliczonymi profilowaniami zainienia w poszczególnych otworach; Ma – strop ewaporatów badenu, Kstr – strop utworów kredy, J3+K1str – strop utworów jury górnej i kredy dolnej, pozostałe skróty – stropy interpretowanych kompleksów wydzielonych w profilu miocenu w poszczególnych otworach

Seismic interpretation of Miocene sediments based on the distinguished lithofacial complexes

The interpretation was based on an analysis of seismic attributes, which was very helpful in more detailed structural interpretation. In view of this, the most useful attributes were: RMS Amplitude, Time Gain, Dominant Frequency, Relative Acoustic Impedance, First Derivative, Sweetness, Variance (Edge Method).

This seismic interpretation supported by well logs analysis clearly indicates a high facies variability of investigated Miocene autochthonous strata within the analysed 3D seismic survey. Generally, the distinguishable sandstone interbeds most often appear in the lower part of the profile, whereas in the upper part the fine-grained and thin-layered deposits prevail. Additionally, during the analysis of the seismic survey, various discontinuity surfaces of different origins were found. They can be connected with sudden facies changes (for example with the presence of channel zones), with submarine erosion and also with synsedimentary tectonics. A great part of the above discontinuities has the nature of angular unconformity surfaces. The presence of angular unconformities of that type and the appearance of local progradation systems and com-

pression deformation zones in the Miocene strata of the central part of the Carpathian Foredeep has also been remarked on by other authors, among others Kirchner and Połtowicz (1974), Krzywiec (2001, 2006), Krzywiec et al. (2004).

The profiles of the “O” and “J” boreholes, situated above the horst zone of the Mesozoic basement are generally characterized by the highest similarity of facies succession (fig. 8). The only exception are the bottom parts of both profiles (below the sandstone complexes distinguished in boreholes O_p3 and J_p2), considerably different in terms of lithology. Borehole “ZA” situated on the NE slope of the mentioned zone is characterized by the highest facies variability, displayed in the presence of numerous alternating sandstone interbeds, mudstone or heterolithic complexes (fig. 7). The last of the interpreted boreholes “ZU” is located in the tectonically lowered zone in the SW part of the survey where the thickness of the Miocene sediments is significantly higher than in the other analysed boreholes (fig. 8). The lowest part of the Miocene profile in this zone shows a definitely lower clay content than in other boreholes, and sandstone complexes appearing in this zone are being successively pinched out in the NE direction, which is connected with the mentioned basement elevation in that zone.

The outstanding element in the profile of the borehole "O" is an interbed of sandstones separated by a mudstone set. Both propagation and character of the sandstone complexes seismic record (horizons O_p1 and O_p3 fig. 8) indicate that they can be sediments of channel facies appearing in the milieu of fine grained clastics. The above thesis is justified mainly by characteristic for that type of sediments sharp contact of the bottom surface of this complex, revealing a sudden lithological change, shown in the image of chosen seismic attributes. The shape of the presumable channel zone was best reflected in the version of Relative Acoustic Impedance attribute (fig. 9), where also the edge zones of the presumable channel were emphasized, since that attribute has been designed to detect different types of angular unconformities and sequence boundaries (Azevedo and Pereira, 2009). A sudden change of lithology in the shape of a sharp contact of the deposits with a high clay content of the heterolithic complex O_h4 and the situated above sandstones of the O_p3 complex can be seen on the well logs, for example the gamma ray log (fig. 10). Thus, the erosive nature of that surface is highly probable.

As for the investigated Miocene rocks, the natural gas saturation zone located within the O_m3 complex has also been distinctly displayed in the log of the mentioned attribute. It appears as the contrasting, positive and negative values of RAI attribute (ellipse no. 1 in fig. 9.). The natural gas flow of circa 50 m³/min was obtained out of this interval. The interval in which hydrocarbon saturation was indicated on the basis of well logs interpretation (fig. 10), perfectly correlates in the seismic image with the amplitude gain (bright spot), what can be best seen in the version of the Time Gain attribute (figs 11, 12). Although direct indicators of hydrocarbon saturation (DHI), especially those of the bright spot type, are usually characteristic mainly for natural gas saturated sandstones of high porosity (among others Castanga et al., 1995; Borys, 1996; Pietsch et al., 1998; Roden et al., 2005; Nanda, 2016; He et al., 2017), in the analysed rocks of the mudstone complex, a rise of amplitude in the gas saturated zone is also clearly visible. Within the interpreted O_m3 complex, several objects of similar seismic record but unrecognized by drilling (ellipses no. 2–4 in figures 11, 12) can be distinguished. They are characterized by a rise of amplitude and, at the same time,

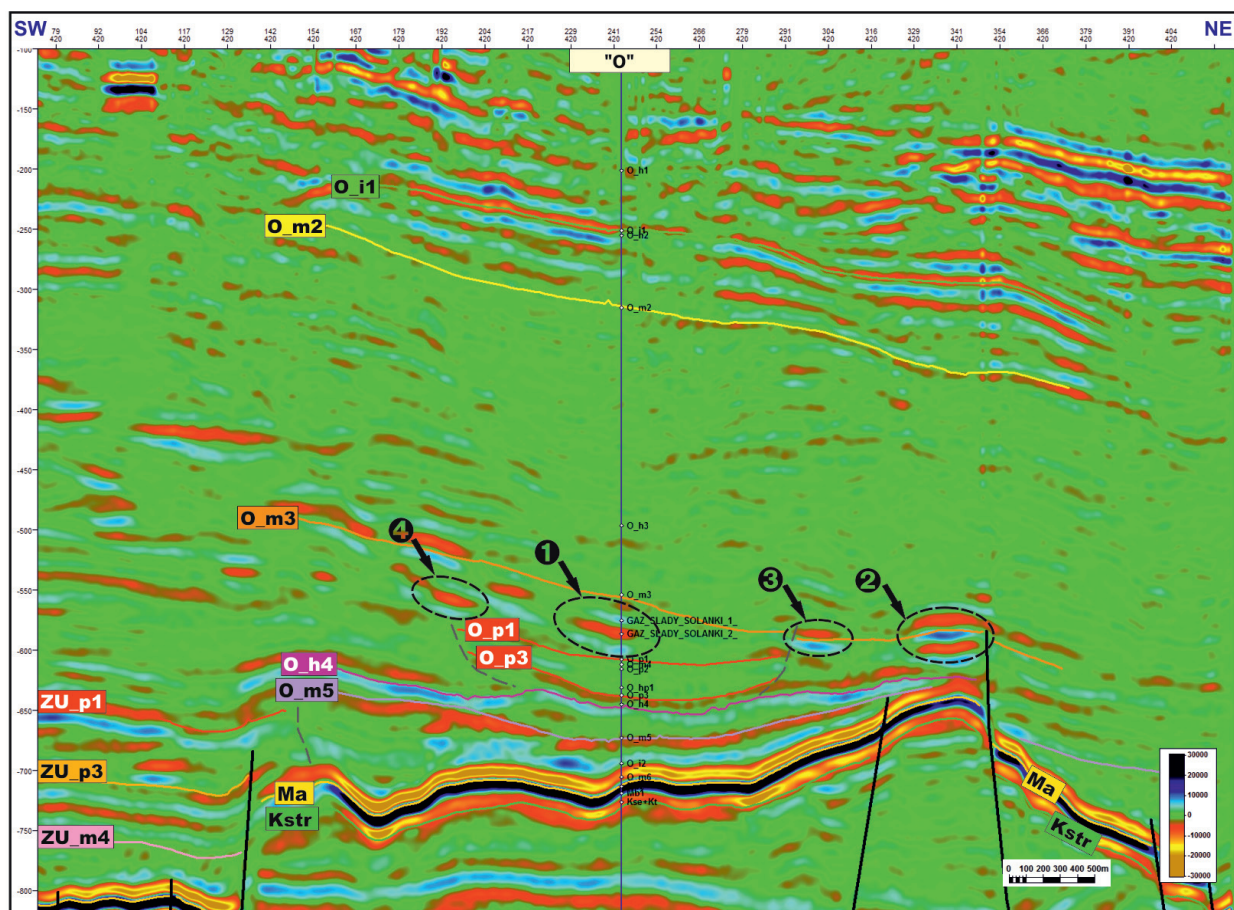


Fig. 9. Seismic time section X420 in a version of the Relative Acoustic Impedance attribute; 1 – zone of natural gas saturation in the region of the „O” borehole, 2–4 other objects presumably gas saturated, undrilled

Rys. 9. Czasowy przekrój sejsmiczny X420 w wersji atrybutu *Relative Acoustic Impedance*; 1 – strefa nasyconego gazem ziemnym w rejone otworu „O”, 2–4 – pozostałe obiekty przypuszczalnie nasycone gazem, nierozpoznane wiertniczo

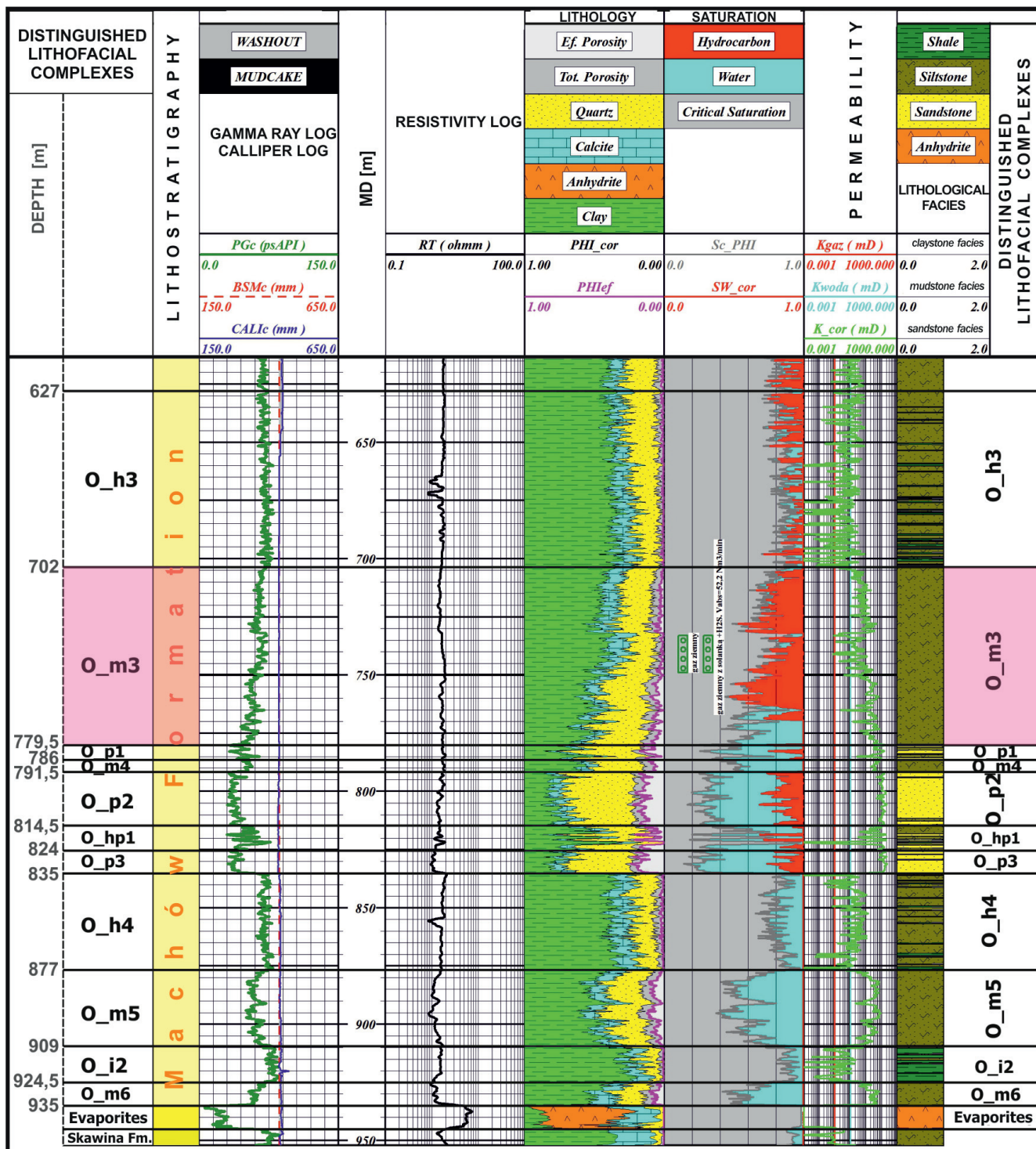


Fig. 10. Distinguished complexes in the lower part of the Miocene sediments profile in the borehole „O”

Rys. 10. Wydzielenia kompleksów fazowych w niższej części profilu utworów miocenu w otworze „O”

a drop of frequency (fig. 13) in relation to the surrounding sediments. A detailed range of the discussed zones can be also traced based on the First Derivative attribute helpful for interpretation of thin-layered sequences. That attribute provides considerably greater continuity and sharpness of seismic reflexes, and that results in a better amplitude – lithology correlation (Zeng and Backus, 2005a, 2005b; Bartoń and Urbaniec, 2018).

The ellipse encircled zone number 6 in figure 12 represents the natural gas saturated interval selected within the J_m3 mudstone complex in borehole “J” (fig. 15). After perforation, a flow of gas of above 56 m³/min together with inflow of brine (with water ratio 1141–2035 g/m³) was obtained. It should be notified that within the discussed zone, the amplitude values are significantly higher in relation to the gas interval recognized in the “O” borehole, reflected, among others, in the image of the First

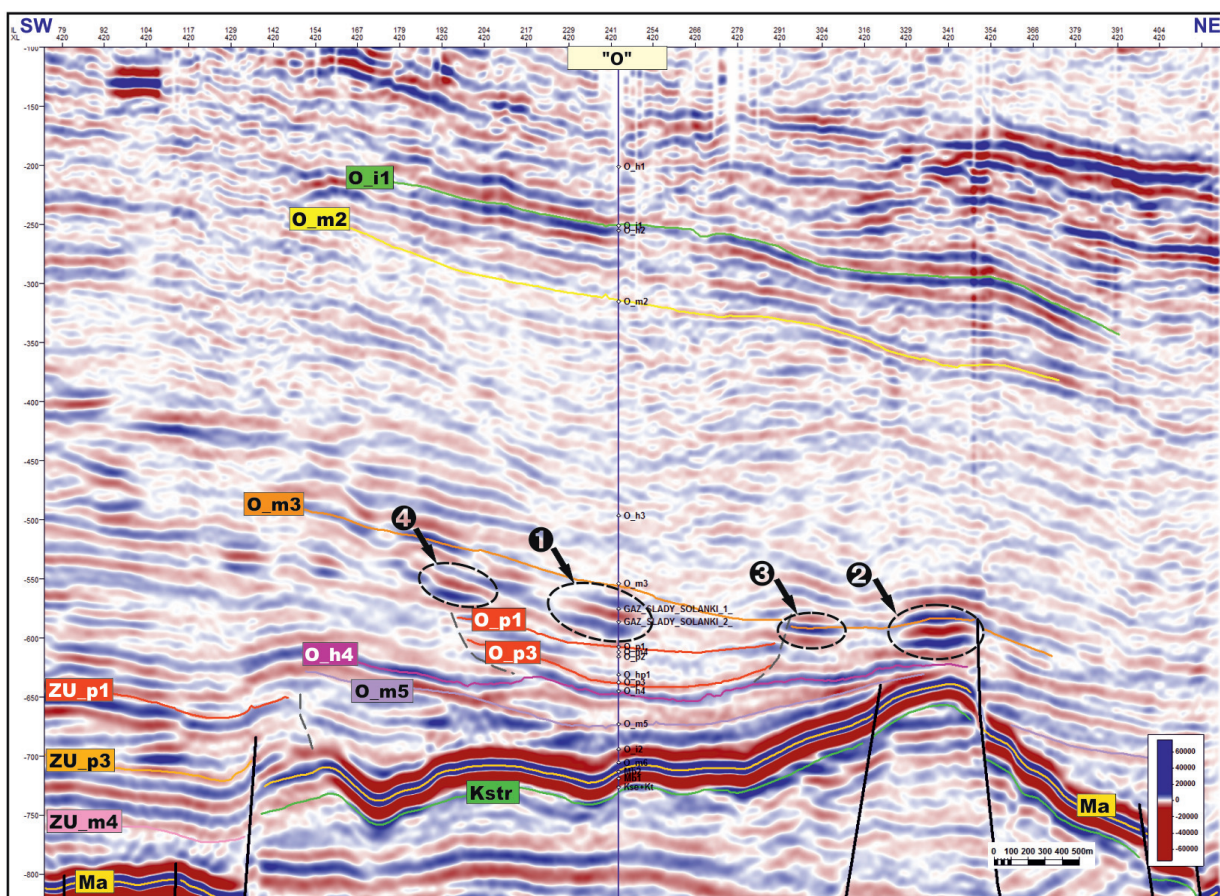


Fig. 11. Seismic time section X420 in the version of Time Gain attribute; 1 – natural gas saturated zone in the region of the „O” borehole, 2–4 remaining objects, presumably gas saturated, unrecognized by drilling

Rys. 11: Czasowy przekrój sejsmiczny X420 w wersji atrybutu *Time Gain*; 1-strefa nasycona gazem ziemnym w rejonie otworu „O”, 2–4 – pozostałe obiekty przypuszczalnie nasycone gazem, nieroznajomione wiertniczo

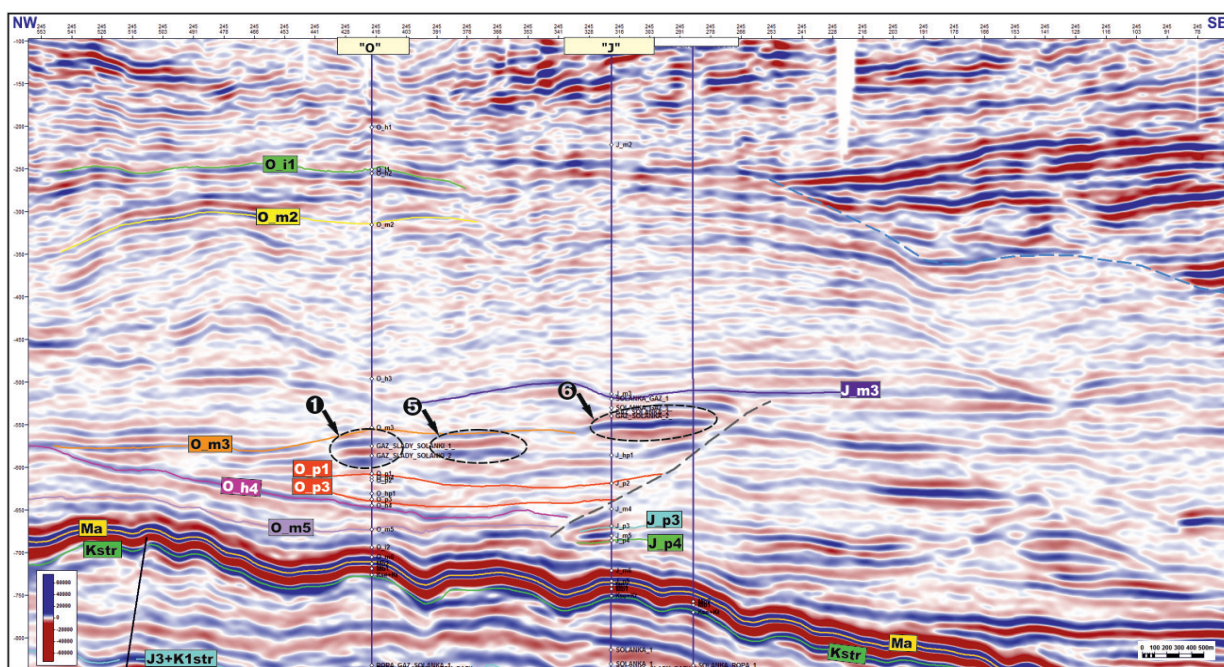


Fig. 12. Seismic time section L245 in the version of the Time Gain attribute; 1 – natural gas saturated zone in the region of the „O” borehole, 5 – presumably a gas saturated zone, unrecognized by drilling, 6 – gas and brine saturated zone recognized in the „J” borehole

Rys. 12. Czasowy przekrój sejsmiczny L245 w wersji atrybutu *Time Gain*; 1 – strefa nasycona gazem ziemnym w rejonie otworu „O”, 5 – strefa przypuszczalnie nasycona gazem, nieroznajomiona wiertniczo, 6 – strefa nasycona gazem i solanką, rozpoznana w otworze „J”

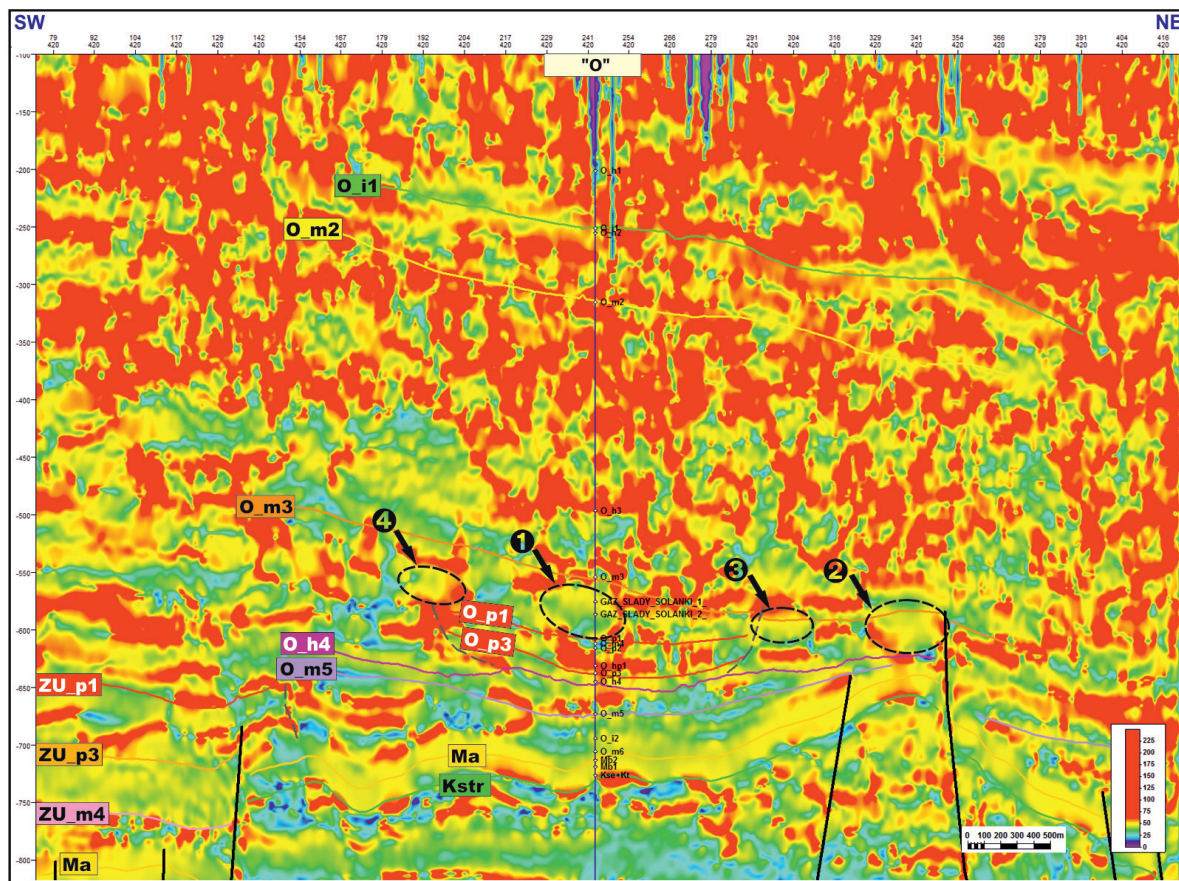


Fig. 13. Seismic time section X420 in the version of the Dominant Frequency attribute; 1 – natural gas saturated zone in the region of the “O” borehole, 2–4 remaining objects, presumably gas saturated, unrecognized by drilling

Rys. 13. Czasowy przekrój sejsmiczny X420 w wersji atrybutu *Dominant Frequency*; 1 – strefa nasycona gazem ziemnym w rejonie otworu „O”, 2–4 – pozostałe obiekty przypuszczalnie nasycone gazem, nierozpoznane wiertniczo

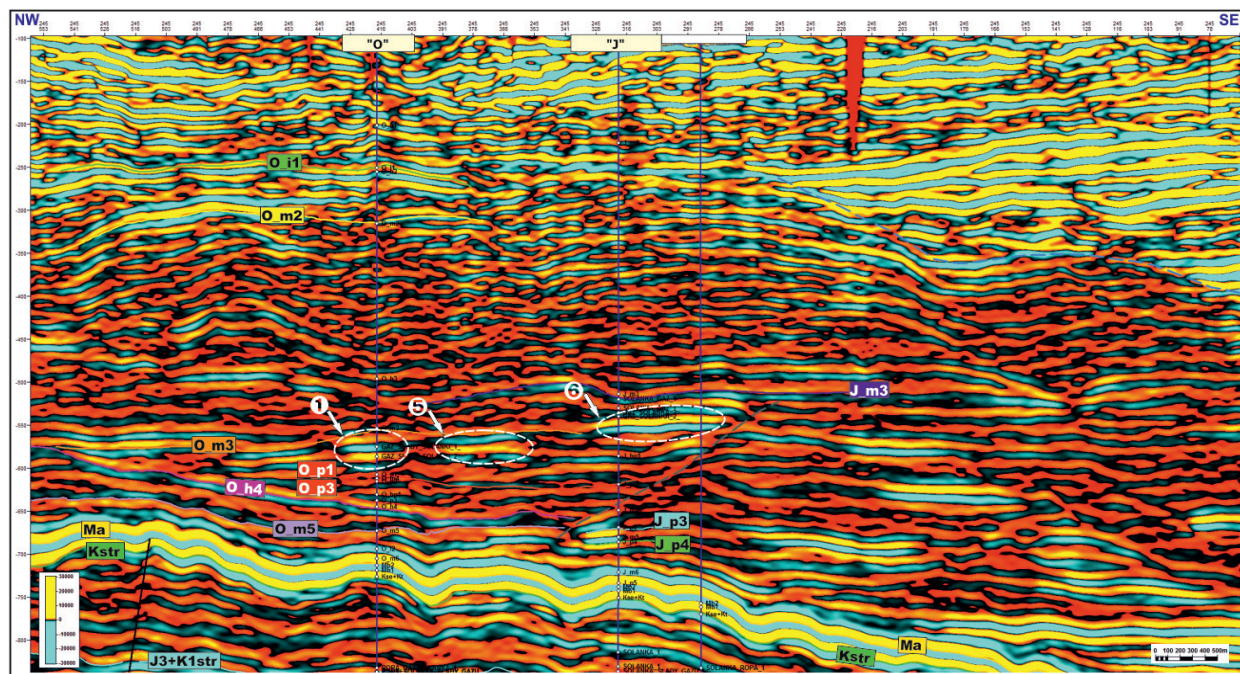


Fig. 14. Seismic time section L245 in the version of the First Derivative attribute; 1 – natural gas saturated zone in the region of the “O” borehole, 5 – presumably a gas saturated zone, unrecognized by drilling, 6 – gas and brine saturated zone, recognized by drilling in the “J” borehole

Rys. 14. Czasowy przekrój sejsmiczny L245 w wersji atrybutu *First Derivative*; 1 – strefa nasycona gazem ziemnym w rejonie otworu „O”, 5 – strefa przypuszczalnie nasycona gazem, nierozpoznana wiertniczo, 6 – strefa nasycona gazem i solanką, rozpoznana w otworze „J”

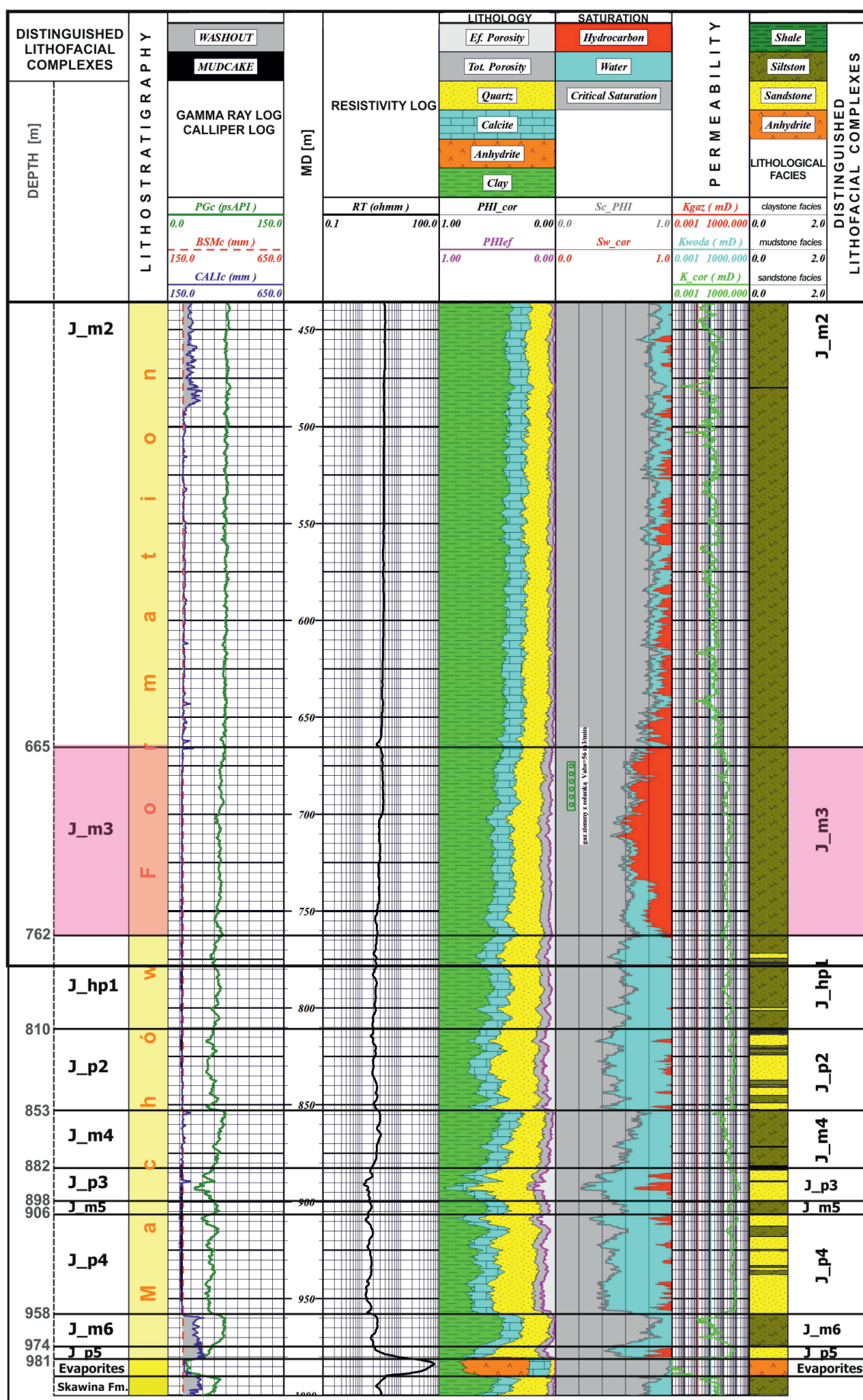


Fig. 15. Complexes distinguished in the lower part of the Miocene sediments profile, in the "J" borehole
Rys. 15. Wydzielenia kompleksów fazjalnych w niższej części profilu utworów miocenu w otworze „J”

Derivative attribute (fig. 14) as considerably stronger contrast between the discussed zone and its surroundings. The difference in seismic image of both objects recognized within the “O” and “J” boreholes can be a result of several factors, such as: internal lithological diversity of the investigated mudstone complexes, accumulation range, differences in saturation (relation of the value of hydrocarbon saturation to water saturation), and also different thickness of complexes as well as of hydrocarbon saturated zones. Based on the analysed material, it is difficult to establish which of the mentioned factors would be decisive in this case.

The differences in lithology of natural gas saturated complexes in the mentioned boreholes are comparatively slight (figs 10, 15) because both complexes become more fine-grained towards the upper part of the profile, and also both of them represent a transition from sediments of a higher sand content to the overlying sediments of a higher clay content. Although the profile of the O_m3 complex may appear lithologically more diverse (containing greater amounts of fine sandstone or clay interbeds) in comparison to the J_m3 complex, most probably it is only because in the “O” borehole, probes of greater vertical resolution were applied.

The J_m3 mudstone complex displays greater thickness (97 m) in relation to the O_m3 complex (77.5 m) but a direct comparison of thicknesses of natural gas saturated zones in both boreholes allows to state that the difference is no more than a few meters (figs 10, 15). Thus thickness is a factor not significant enough to considerably influence the seismic record.

Hence it can be assumed that the most significant factors that can differentiate the seismic record are: the size of potential traps for hydrocarbon accumulation and also the difference (maybe slight) in reservoir media saturation. The surface of the zone characterized with an anomaly of seismic record in the region of the “J” borehole is definitely larger than that of an object in the region of the “O” borehole, which can be best seen on time slices in the version of the Sweetness attribute (compare object 6 in fig. 16A and object 1 in fig. 16B). Still, when considering the difference in reservoir media saturation, even if it appears as slight, it is distinctly noticeable. In the “O” borehole, the porous space in the upper part of the mudstone complex O_m3 is generally 100% natural gas saturated (fig. 10), but in the J_m3 complex of the “J” borehole also a partial reservoir water saturation can be noticed (fig. 15).

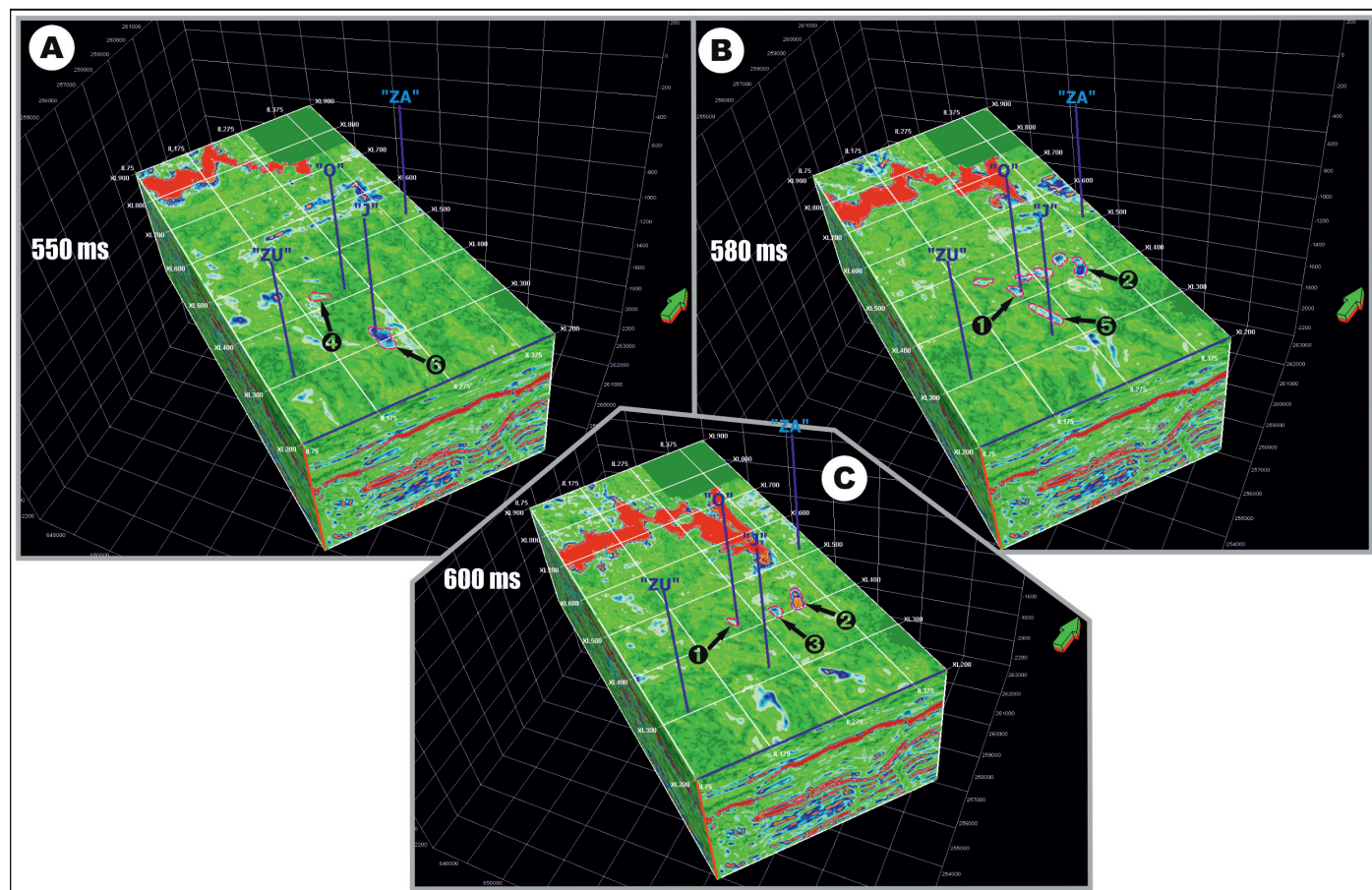


Fig. 16. Comparison of the image of the Sweetness attribute for three time slices: A – 550 ms, B – 580 ms, C – 600 ms; objects’ numeration corresponds to that of the seismic time section (figs 9, 11–14)

Rys. 16. Porównanie obrazu atrybutu *Sweetness* dla trzech poziomowych przekrojów czasowych: A – 550 ms, B – 580 ms, C – 600 ms; numeracja obiektów odpowiada ich numeracji na przekrojach sejsmicznych (rys. 9, 11–14)

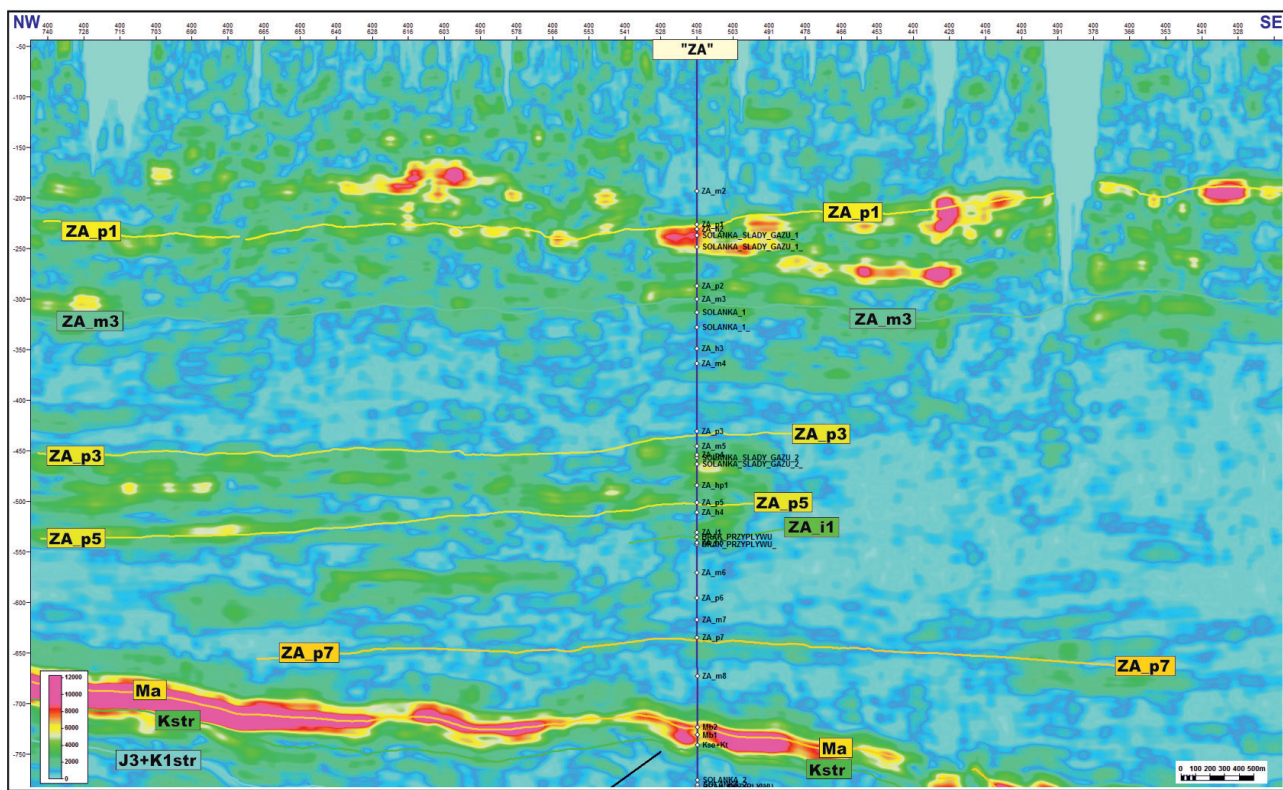


Fig. 17. Seismic time section L400 in the version of the RMS Amplitude attribute

Rys. 17. Czasowy przekrój sejsmiczny L400 w wersji atrybutu *RMS Amplitude*

The profile of the “ZA” borehole significantly differs from those in the central part of the seismic survey, as characterized with considerably higher facies diversity. The complexes distinguished in the higher part of the profile propagate mainly in NW and SE directions, that is parallel to the extent of the horst zone occupying the central part of the analysed seismic survey. However, in the SW direction they undergo rapid pinching out into a large angular unconformity surface of regional scale, displayed within the Miocene formations and situated above the tectonic edge of the mentioned horst zone developed within the Mesozoic basement (fig. 8). The origins of this surface most probably can be connected with both the synsedimentary tectonics and reactivation of older dislocation zones. That reactivation was probably an effect of rotation of basement blocks, resulting from tensions caused by the Carpathian belt, developing and thrusting from the SW direction and the configuration of the Carpathian Foredeep sedimentary basin changing with time.

The seismic image in the region of “ZA” borehole correlates very well with the interpretation of the well logs (fig. 7). Packages of high amplitude, continuous reflections correspond to sandstone complexes (from ZA_p1 to ZA_p5) (fig. 17), most often of very good reservoir parameters and containing gas-saturated brines. Only the sandstone packages of greater thickness appearing in the bottom part of the profile (complexes ZA_p6 and ZA_p7) are less distinctly marked and characterized with definitely lower record dynamics (fig. 17) with, at

the same time, distinct continuity of reflections. In the middle part of the Miocene profile in the region of the “ZA” borehole, a zone of sudden facies changes can be observed, within which the correlated horizons connected with the tops of complexes ZA_p3, ZA_p5, and ZA_i1 (fig. 17) disappear.

Geological interpretation

The presence of numerous discontinuity surfaces interpreted in the seismic image, in their major part being erosion surfaces of sediments deposited in the earlier phases, is probably connected with the configuration of the Carpathian Foredeep sedimentary basin changing with time, including the northwards dislocation of its axis. The migration of depocentres in the basin was most probably accompanied by rotation of blocks in the basement of the Carpathian Foredeep as well as the reactivation of older dislocation zones (vide Krzywiec, 1997, 2001; Porębski, 1999; Oszczypko, 2006; Jipa, 2018).

The image on the horizontal seismic profiles indicates the presence of an extended delta system, or, more probably, of its distal part characterized by prevalence of finer sediments. That system is very well reflected on the 520 ms time slice in the versions of the Variance (Edge Method) and Time Gain (fig. 18) attributes. Especially important is the Variance attribute using local variance as a measurement of seismic signal inconsistency

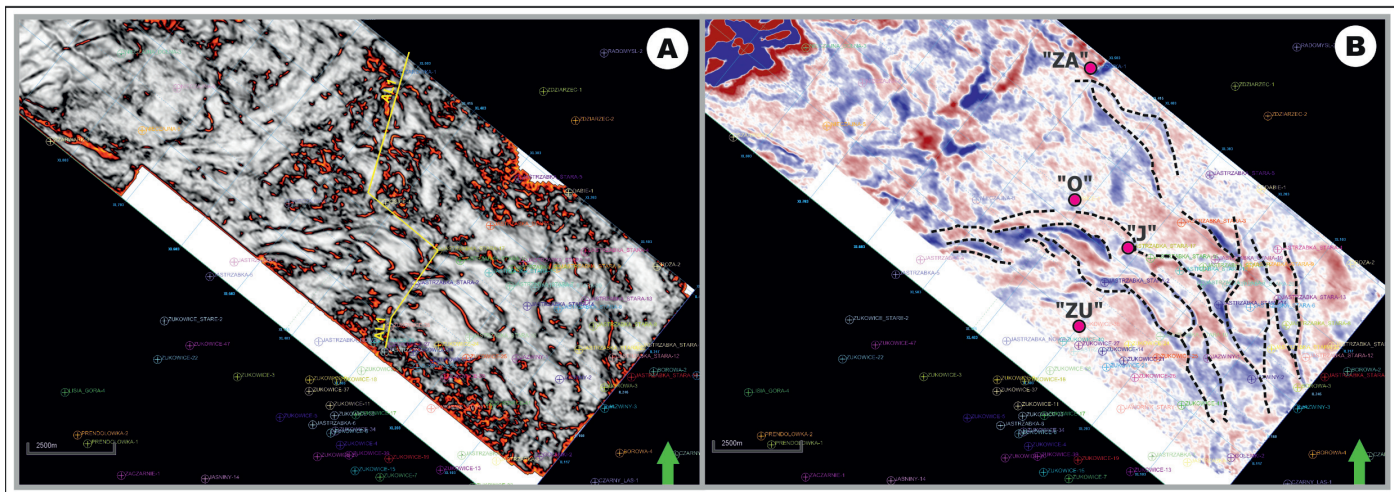


Fig. 18. Seismic time slice (520 ms); A – in the version of the Variance attribute; B – in the version of the Time Gain attribute with interpretation

Rys. 18. Czasowy przekrój poziomy (520 ms): A – w wersji atrybutu *Variance*, B – w wersji atrybutu *Time Gain* z interpretacją

(Randen et al., 2001). It is applied in detecting various discontinuity zones, such as faults, angular unconformities or boundaries of depositional sequences.

Geological interpretation is considerably hindered by a very small scope of the coring of the Miocene formations but it can be assumed that in the investigated area, in the lower part of the Miocene profile we are dealing mainly with more distal elements of the delta system developing during that time. Similar lithofacies are known from the Miocene profiles of other regions of the Carpathian Foredeep (for example Dziadzio, 2000; Porebski et al., 2003; Myśliwiec, 2004; Porebski and Warchał, 2006; Puskarczyk et al., 2015; Marzec et al., 2016). We are probably dealing here with a diversified sequence of sediments, starting with prodelta formations (dominated by mudstone sedimentation), through heterolithic complexes of distal delta-lobes locally, to sandstones and mudstones of stream-mouth bars and distributary channel zones. The high thickness of the heterolithic segment containing sandy or sandy/silty turbidite sand hyperpycnites is a characteristic feature of Miocene deltas of the Carpathian Foredeep (Porebski and Warchał, 2006; Paszkowski et al., 2009).

The conducted analyses, especially the determination of facies localization and arrangement of particular elements of the deposition system, indicate that the deposited material was transported from the SW direction, from the region of the then uplifting Carpathian orogen.

Summary

The above analysis of the well logs and seismic data allowed for a more detailed seismic and geological interpretation of the investigated area.

An important aspect of this work was the possibility of detecting natural gas saturated zones on the basis of an analysis of the seismic image and logging data available in the investigated region. Attempts to define the degree of Miocene rocks saturation with natural gas by basing on seismic modelling were carried out by, among others, Pietsch and Tatarata (2008), Pietsch et al. (2008) and Tatarata and Pietsch (2008). These authors concluded that because of such high lithofacial changeability of the Miocene formations and the considerable diversity range of petrophysical parameters, and also the limited amount of available well logs and seismic data, the assumed seismogeologic models are only an approximate reconstruction of the true relations between the seismic anomalies and the degree of the porous space gas saturation.

In the case of the presented topic, the gas or gas and brine saturated zones documented in the analysed boreholes, known from formation tests, despite their usually small spatial extent, can be identified on the seismic record. The conducted studies have shown that in the case of rocks of low reservoir parameters (mudstones – very fine grained sandstones), the most significant factors which can result in diversity in the seismic record are the size of potential traps for hydrocarbons accumulation and also the difference (even slight) in reservoir media saturation. However, because of high lithologic diversity and a considerable range of changeability of particular parameters, it is not possible to reliably indicate, by basing on only a seismic record, which of the analysed objects are saturated with natural gas and which are saturated with gas and brine.

A set of fine grained clastic sediments (mainly mudstones or heterolithic beds in the lower part of the Miocene profile, in which the following complexes were distinguished: O_m3 (the “O” borehole), J_m3 (the “J” borehole) and ZU_m2 (the “ZU” borehole) has been accepted as the most interesting for pros-

pecting purposes. Within that package, several potential natural gas saturated objects (figs 9, 11–14) have been interpreted.

This paper was written on the basis of the statutory work entitled: *Uszczegółowienie interpretacji sejsmicznej w obszarze zapadliska przedkarpackiego na podstawie kompleksowej analizy pomiarów geofizyki otwórowej* – the works of the Oil and Gas Institute – National Research Institute was commissioned by the Ministry of Science and Higher Education; order number: 0032/SR/2018, archive number: DK-4100-32/2018.

References

- Alexandrowicz S.W., Garlicki A., Rutkowski J., 1982. Podstawowe jednostki litostratigraficzne miocenu zapadliska przedkarpackiego. *Kwartalnik Geologiczny*, 26(2): 470–471.
- Azevedo L., Pereira G.R., 2009. Seismic attributes in hydrocarbon reservoir characterization. *Wyd. Universidade de Aveiro, Departamento de Geociências, Aveiro*: 1–165.
- Bartoń R., Urbaniec A., 2018. Wykorzystanie pomiarów PPS do uszczegółowienia interpretacji sejsmicznej 3D na przykładzie utworów dolnego paleozoiku. *Nafta-Gaz*, 9: 655–668. DOI: 10.18668/NG.2018.09.04.
- Borys Z., 1996. Aktualne problemy poszukiwań węglowodorów we wschodniej części przedgórza Karpat. *Przegląd Geologiczny*, 44(10): 1019–1023.
- Brewer R.J., 2002. VSP Data in Comparison to the Check Shot Velocity Survey. *Search and Discovery Article No 40059, Houston, Halliburton Energy Services*. <http://www.searchanddiscovery.com/documents/geophysical/brewer/index.htm>.
- Bukowski K., 2011. Badeńska sedymentacja salinarna na obszarze między Rybnikiem a Dębicą w świetle badań geochemicznych, izotopowych i radiometrycznych. *Rozprawy i monografie, Wydawnictwa AGH, Kraków*, 236: 1–184.
- Buła Z., Żaba J., Habryn R., 2008. Regionalizacja tektoniczna Polski – Polska południowa (blok górnouślaski i małopolski). *Przegląd Geologiczny*, 56(10): 912–920.
- Castagna J.P., Han D.H., Batzle M.L., 1995. Issues in rock physics and implications for DHI interpretation. *The Leading Edge*, 14(8): 883–886.
- Dziadzio P., 2000. Sekwencje depozycyjne w utworach badenu i sarmatu w SE części zapadliska przedkarpackiego. *Przegląd Geologiczny*, 48(12): 1124–1138.
- He Y., Zhu J.T., Zhang Y.Z., Liu A.Q., Pan G.C., 2017. The Research and Application of Bright Spot Quantitative Interpretation in Deepwater Exploration. *Open Journal of Geology*, 7: 588–601. DOI: 10.4236/ojg.2017.74040.
- Jarzyna J., Krakowska P., 2010. Dobór parametrów petrofizycznych węglanowych skał zbiornikowych w celu podwyższenia dokładności wyznaczania współczynnika nasycenia wodą. *Nafta-Gaz*, 7: 547–556.
- Jipa D.C., 2018. Large-scale along-arc sedimentary migration in the Carpathian Foredeep. A paleogeographic approach. *Palaeogeography, Palaeoclimatology, Palaeoecology*, 505: 140–149. DOI: 10.1016/j.palaeo.2018.05.037.
- Karnkowski P., 1993. Złoża gazu ziemnego i ropy naftowej w Polsce. Tom 2 Karpaty i zapadlisko przedkarpackie. *Wyd. Towarzystwo Geosynoptyków „Geos” AGH*.
- Kirchner Z., Połtowicz S., 1974. Budowa geologiczna obszaru między Brzeskiem a Wojniczem. *Rocznik Pol. Tow. Geol.*, 44(2–3): 293–320.
- Krzywiec P., 1997. Large-scale tectono-sedimentary Middle Miocene history of the central and eastern Polish Carpathian Foredeep Basin – results of seismic data interpretation. *Przegląd Geologiczny*, 45(10): 1039–1053.
- Krzywiec P., 2001. Contrasting tectonic and sedimentary history of the central and eastern parts of the Polish Carpathians Foredeep Basin – results of seismic data interpretation. *Marine and Petroleum Geology*, 18: 13–38.
- Krzywiec P., 2006. Geodynamiczne i tektoniczne uwarunkowania ewolucji basenów przedgórkowych, z odniesieniami do zapadliska przedkarpackiego. *Przegląd Geologiczny*, 54(5): 404–412.
- Krzywiec P., Aleksandrowski P., Florek R., Siupik J., 2004. Budowa frontalnej strefy Karpat zewnętrznych na przykładzie mioceńskiej jednostki Zgłobie w rejonie Brzeska-Wojnicza – nowe dane, nowe modele, nowe pytania. *Przegląd Geologiczny*, 52(11): 1051–1059.
- Marzec P., Sechman H., Kasperska M., Cichostepski K., Guzy P., Pietsch K., Porębski S.J., 2016. Interpretation of a gas chimney in the Polish Carpathian Foredeep based on integrated seismic and geochemical data. *Basin Research*, (2016): 1–18. DOI: 10.1111/bre.12216.
- Montaron B., 2008. Connectivity theory – a new approach to modeling “non-archie” rocks. *SPWLA 49th Annual Logging Symposium, May 25–28*.
- Montaron B., 2009. Connectivity theory – a new approach to modeling non-archie rocks. *Petrophysics*, 50(2): 102–115.
- Myśliwiec M., 2004. Mioceńskie skały zbiornikowe zapadliska przedkarpackiego. *Przegląd Geologiczny*, 52(7): 581–592.
- Nanda N.C., 2016. Seismic Data Interpretation and Evaluation for Hydrocarbon Exploration and Production: a Practitioner’s Guide. *Wyd. Springer International Publishing Switzerland*. DOI: 10.1007/978-3-319-26491-2.
- Olszewska B., 1999. Biostratygrafia neogenu zapadliska przedkarpackiego w świetle nowych danych mikropaleontologicznych. *Prace Państw. Inst. Geol.*, 168: 9–28.
- Oszczyzko N., 2006. Powstanie i rozwój polskiej części zapadliska przedkarpackiego. *Przegląd Geologiczny*, 54(5): 396–403.
- Paszkowski M., Porębski S.J., Warchał M., 2009. Koncepcja projektu otworu kierunkowego w mioceńskich utworach zapadliska przedkarpackiego. *Wiadomości Naftowe i Gazownicze*, 3(131): 4–13.
- Pietsch K., Dereń D., Gąsiorowski T., 1998. Anomalie sejsmiczne wywołane wielopoziomowymi złożami gazu w północno-wschodniej części zapadliska przedkarpackiego. *Przegląd Geologiczny*, 46(8): 676–684.
- Pietsch K., Nawieśniak A., Kobylarski M., Tatarata A., 2008. Czy tłumienie fal sejsmicznych może być źródłem informacji o stopniu nasycenia skał zbiornikowych gazem? — studium modelowe. *Przegląd Geologiczny*, 56(7): 545–551.
- Pietsch K., Tatarata A., 2008. Wykorzystanie atrybutów bazujących na danych sejsmicznych przed składaniem do oceny stopnia nasycenia gazem warstw złożowych, NE część zapadliska przedkarpackiego. *Geologia (Kwartalnik AGH)*, 34(2): 301–320.
- Porębski S.J., 1999. Środowisko depozycyjne sukcesji nadewaporowej (górny baden) w rejonie Kraków – Brzesko (zapadlisko przedkarpackie). *Prace Państw. Inst. Geol.*, 168: 97–118.
- Porębski S.J., Pietsch K., Hodak R., Steel R.J., 2003 – Origin and sequential development of Badenian-Sarmatian clinoforms in the Carpathian Foreland basin (SE Poland). *Geologica Carpathica*, 54(2): 119–136.
- Porębski S.J., Warchał M., 2006. Znaczenie przepływów hiperynalnych i klinoform deltowych dla interpretacji sedymentologicznych formacji z Machowa (miocen zapadliska przedkarpackiego). *Przegląd Geologiczny*, 54(5): 421–429.

- Puskarczyk E., Jarzyna J., Porębski S.J., 2015. Application of multi-variate statistical methods for characterizing heterolithic reservoirs based on wire line logs – example from the Carpathian Foredeep Basin (Middle Miocene, SE Po land). *Geological Quarterly*, 59(1): 157–168. DOI: 10.7306/gq.1202.
- Randen T., Pedersen S. I., Sønneland L., 2001. Automatic extraction of fault surfaces from three-dimensional seismic data. *71st Annual International Meeting, SEG, Expanded Abstracts*: 551–554.
- Roden R., Forrest M., Holeywell R., 2005. The impact of seismic amplitudes on prospect risk analysis. *The Leading Edge*, 7: 706–711.
- Tatarata A., Pietsch K., 2008. Porównanie wybranych atrybutów AVO w poszukiwaniach węglowodorów na przykładzie złoża Łukowa – miocen zapadliska przedkarpackiego. *Prace Instytutu Nafty i Gazu*, 150: 145–152.
- Zeng H., Backus M., 2005a. Interpretive advantages of 90°-phase wavelets: Part 1 – Modeling. *Geophysics*, 70(3): C7–C15.
- Zeng H., Backus M., 2005b. Interpretive advantages of 90°-phase wavelets: Part 2 – Seismic Applications. *Geophysics*, 70(3): C17–C24.



Andrzej URBANIEC Ph.D.
Assistant Professor
Head of the Seismic Department
Oil and Gas Institute – National Research Institute
25 A Lubicz St.
31-503 Krakow
E-mail: andrzej.urbaniec@inig.pl



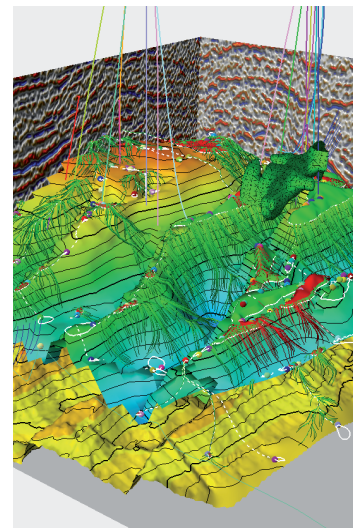
Marek STADTMÜLLER M.Sc. Eng.
Chief Engineering and Technical Specialist
at the Department of Geology and Geochemistry
Oil and Gas Institute – National Research Institute
25 A Lubicz St.
31-503 Krakow
E-mail: marek.stadtmauller@inig.pl



Robert BARTOŃ Ph.D. Eng.
Assistant Professor at the Seismic Department
Oil and Gas Institute – National Research Institute
25 A Lubicz St.
31-503 Krakow
E-mail: robert.barton@inig.pl

OFERTA BADAWCZA ZAKŁADU SEJSMIKI

- przetwarzanie danych sejsmicznych Prestack i Postack;
- przetwarzanie i interpretacja pionowych profilowań sejsmicznych PPS 1C / 3C;
- modelowanie sejsmiczne na danych 2D / 3D;
- interpretacja danych sejsmicznych 2D, 3D oraz pomiarów sejsmiki otworowej PPS-3C;
- interpretacja strukturalna i litofacialna danych sejsmicznych 2D i 3D;
- budowa modeli przedkościowych w domenie czasu i głębokości (na podstawie danych sejsmicznych i geofizyki otworowej) na potrzeby konwersji czas-głębokość oraz migracji głębokościowej;
- podwyższenie rozdzielczości pionowej danych sejsmicznych przy wykorzystaniu pomiarów PPS;
- poprawa rozdzielczości danych sejsmicznych z wykorzystaniem procedury dekompozycji spektralnej;
- konstrukcja map powierzchniowych w domenie czasu i głębokości;
- opracowanie i analiza map atrybutów sejsmicznych, inwersji sejsmicznej, dekompozycji spektralnej;
- wieloatrybutowa charakterystyka ośrodka geologicznego;
- analizy sejsmiczne AVO, AVAZ;
- obliczanie inwersji symultanicznej oraz stochastycznej na danych sejsmicznych;
- identyfikacja anizotropii typu HTI w ośrodku geologicznym przy użyciu danych sejsmicznych i otworowych (określenie intensywno oraz azymutu anizotropii);
- obliczanie parametrów anizotropii typu VTI i HTI oraz określenie głównych kierunków szczelinowości na podstawie wieloazymutalnego pomiaru PPS 3C i pomiarów sejsmicznych 3D;
- wyznaczanie obszarów perspektywicznych dla formacji łupkowych (sweet spots) oraz wskaźników DHI dla złóż konwencjonalnych na danych sejsmicznych;
- prognozowanie ciśnień porowych na podstawie danych sejsmicznych i geofizycznych;
- interpretacja parametrów petrofizycznych w przestrzeni oktotootworowej w oparciu o pomiary pionowego profilowania sejsmicznego (PPS);
- kompleksowa interpretacja geologiczno-złożowa w oparciu zintegrowane dane geologiczne i geofizyczne (analiza cech makroskopowych rdzeni wiertniczych, objawy i wyniki prób złożowych, profilowania geofizyki otworowej, interpretacja sejsmiczna).



Kierownik: dr Andrzej Urbaniec Adres: ul. Bogrowa 1, 30-733 Kraków
Telefon: 12 617 74 86 Faks: 12 653 16 65 E-mail: andrzej.urbaniec@inig.pl



INSTYTUT NAFTY I GAZU
– Państwowy Instytut Badawczy